

# A reinterpretation of the phase transitions in $\text{Na}_2\text{CO}_3$

Alla Arakcheeva\* and Gervais Chapuis

Ecole Polytechnique Fédérale de Lausanne,  
Institut de Physique de la Matière Complexe,  
BSP, 1015 Lausanne, Switzerland

Correspondence e-mail:  
Alla.Arakcheeva@epfl.ch

Received 22 November 2004  
Accepted 14 October 2005

Based on the structural data of phases  $\alpha$  (hexagonal; 756–972 K),  $\beta$  (monoclinic; 605–751 K),  $\gamma$  (incommensurate, monoclinic; 295 K) and  $\delta$  (lock-in, monoclinic; 110 K) of sodium carbonate,  $\text{Na}_2\text{CO}_3$ , we could draw a parallel between the phase transitions and the evolution of the second coordination sphere of the C atoms. The temperature-dependent structures observed in the  $\beta$  phase are reproduced in the incommensurate  $\gamma$  phase as a modulation wave, which relates to the content of the symmetrically equivalent {110} lattice planes in the  $\alpha$  phase. By decreasing the temperature, the phase transitions are associated with a stepwise increase in the number of Na ions participating in the second coordination sphere of the C atoms. Over the full temperature range, this number increases from 3 to 7. The C–O distances and the mobility of the O atoms depends on the number of Na ions in the vicinity of the C atoms.

## 1. Introduction

Incommensurate structures are conveniently described in the superspace formalism. The obvious advantage is that their structures can recover lattice periodicity, in a space varying between four and six dimensions. If the incommensurate structure is part of a sequence of phases where both commensurate and incommensurate structures can exist, it appears that the theoretical tools are still incomplete in order to give a coherent view of the complete set of phases occurring at various temperatures or pressures. From the theoretical considerations of Parlinski & Chapuis (1993), the fundamental role of the atomic interactions of the second coordination sphere (cation–cation for the anion containing compounds) was shown for the ‘commensurate–incommensurate’ phase transition. Based on the sequences of the temperature-dependent phases of  $\text{Na}_2\text{CO}_3$  (Fig. 1), we would like to illustrate this theoretical prediction and show that the specific cation–cation interactions can be associated with each of the phase transitions which have been identified. In this context, the interaction must be understood in terms of the number of second nearest-neighbour interactions which are characterized by distances smaller than a limiting distance which will be discussed later.

The temperature-dependent phase transitions of  $\text{Na}_2\text{CO}_3$  have been widely studied (Wolff & Tuinstra, 1986; Harris & Salje, 1992; Swainson *et al.*, 1995; Harris & Dove, 1995; Harris *et al.*, 1996; Dušek *et al.*, 2003). The following sequence of phases is supported by precise structural investigations which have been repeatedly confirmed:

(i)  $\alpha$ :  $T = \sim 754\text{--}1000$  K; space group  $P6_3/mmc$ ; 10 refinements were reported by Swainson *et al.* (1995) for different temperatures; unit-cell parameters:  $a = 5.209(2)$  Å and  $c$

varies from 6.454 to 6.676 Å [the values  $a_M = 9.022$  (4) and  $b_M = 5.209 \pm 0.002$  Å refer to the monoclinic setting].

(ii)  $\beta$ :  $T = 605\text{--}754$  K; space group  $C2/m$ ; about 20 refinements were performed by Swainson *et al.* (1995) for different temperatures; unit-cell parameters:  $a = 9.00$  (2),  $b = 5.23$  (2) Å, the  $c$  parameter and monoclinic angle  $\beta$  vary from 6.44 Å and from 90 to 99.33°, respectively.

(iii)  $\gamma$  (incommensurate):  $T = 170\text{--}605$  K; super-space group  $C2/m(\alpha_0\gamma)0s$ ; the study was performed at 295 K (Dušek *et al.*, 2003); unit-cell parameters  $a = 8.920$  (7),  $b = 5.245$  (5),  $c = 6.050$  (5) Å,  $\beta = 101.35$  (8)°,  $\mathbf{q} = [0.182$  (1), 0, 0.322 (1)].

(iv)  $\delta$  (lock-in):  $T \leq 170$  K; space group  $P2_1/n$  [equal to superspace group  $C2/m(\frac{1}{6}\frac{1}{3})0s$ ]; the structural data were obtained at 110 K (Dušek *et al.*, 2003); unit-cell parameters  $a = 8.898$  (7),  $b = 5.237$  (5),  $c = 5.996$  (5) Å,  $\beta = 101.87$  (8)°,  $\mathbf{q} = [\frac{1}{6}, 0, \frac{1}{3}]$ .

In all the available publications, the phase transitions are associated with the tilt of the triangular CO<sub>3</sub> rigid units. However, their origins have been explained in two different ways. The  $\alpha \rightarrow \beta$  structure transformation was associated with a ferroelastic second-order phase transition by Swainson *et al.* (1995), with the spontaneous shear strain (namely, the component  $\epsilon_5 = a \cos \beta^* / a_0$ ) as the primary order parameter. In this model, the carbonate rotation simply follows rather than drives the shear strain. A lattice dynamics calculation based on a C—O and Na—O rigid-bond model was invoked to justify this model. In Dušek *et al.* (2003), the origin of the  $\beta \rightarrow \gamma$  phase transition was associated with the tilting of the carbonate groups. The unsaturated bonding potential of the Na<sup>+</sup> ions was invoked in order to explain the progressive tilt of the CO<sub>3</sub> group. Indeed, the bond-valence sums (BVS) calculated by Dušek *et al.* (2003) demonstrate this tendency for one Na<sup>+</sup> ion [BVS: 0.71 ( $\alpha$ )  $\rightarrow$  0.80 ( $\beta$ )  $\rightarrow$  0.94 ( $\gamma$ )  $\rightarrow$  1.00 ( $\delta$ )]. However, the other two Na<sup>+</sup> ions become over-saturated with Na—O bonds [BVS: 1.06 ( $\alpha$ )  $\rightarrow$  1.25 ( $\beta$ )  $\rightarrow$  1.35 ( $\gamma$ )  $\rightarrow$  1.4 ( $\delta$ )], which is not favorable for the structure stabilization. Hence, the question about the nature of the phase transitions is still open and the origin of the tilt of the CO<sub>3</sub> triangle at lower temperature remains without a plausible explanation.

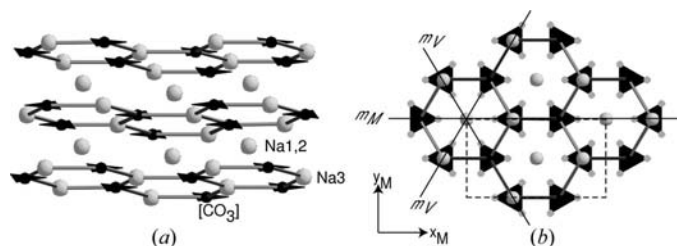


**Figure 1**  
The crystal structure of Na<sub>2</sub>CO<sub>3</sub>: (a) perspective view and (b) the (001) projection. The Na3 and [CO<sub>3</sub>] ions form graphite-like layers, parallel to (001) and stacked in the third direction. The Na1,2 ions are located in the hexagonal channels. The three atomic planes of the {110}<sub>hex</sub> family contain all the atoms of the structure. They are equivalent in the hexagonal  $\alpha$  phase and indicated as  $m_M$  and  $m_V$  corresponding to one mirror plane and two ‘virtual mirror’ planes in the monoclinic modifications. The monoclinic unit cell is shown with a dashed line.

No evidence of any discontinuity at the transition temperatures was mentioned in any of the available publications dedicated to Na<sub>2</sub>CO<sub>3</sub> crystal structures. Only the C—O and Na—O interactions were considered in order to justify the transition mechanism.

In the present article, we show that by decreasing the temperature some dramatic changes occur in this structure between non-O atoms, which are associated with the phase transformations. Based on an analysis of the structural data obtained from Swainson *et al.* (1995) and Dušek *et al.* (2003) for all modifications mentioned above, we postulate that the gradual strengthening of the C—Na interactions (decrease of C—Na distances from 3.4 to  $3.0 \pm 0.1$  Å) is the main structural feature underlying all the phase transitions observed over decreasing temperatures. All the temperature-dependent

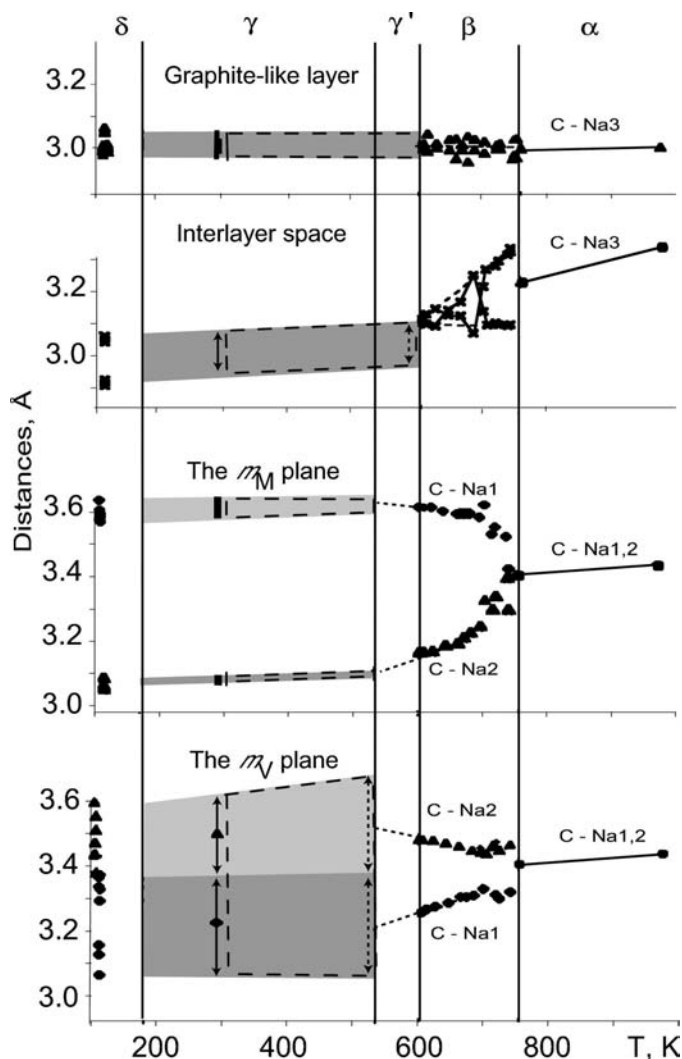


**Figure 2**  
Temperature dependence of the C—Na distances in the 110–972 K range. Various dots and solid lines indicate the experimental data published in Swainson *et al.* (1995) and Dušek *et al.* (2003). The solid vertical lines correspond to the phase transition temperatures. The gray areas indicate modulated distances and the double-sided arrows indicate the anti-phase modulations in the two  $m_V$  planes. The dashed lines are approximations. The incommensurate  $\gamma'$  phase is derived from a reinterpretation of the experimental data.

transformations, such as the increase of the monoclinic  $\beta$  angle (justifying the  $\epsilon_5 = a \cos \beta^*/a_0$  shear strain component), the tilt of the  $\text{CO}_3$  triangles, the difference between the O1 and O2 atomic displacements and the C—O distances, follow directly from the decrease of the C—Na distances on decreasing the temperature. The result is a stepwise formation of C—Na bonds, *i.e.* C—Na distances shorter than 3.1 Å. [It is worth mentioning that the C—Na distances, 2.62–2.92 Å, characteristic of oxygen-free  $\text{Na}_2\text{C}_2$  (Hemmersbach *et al.*, 1999) are close to these values.] We show that each successive phase transition is correlated with the formation of an additional bond in the second coordination sphere of C atoms. The C—Na bond formation is *not* continuous at the  $\alpha \rightarrow \beta$  transition temperature. The  $\alpha \rightarrow \beta$  transformation mechanism is more complex than the description given in Swainson *et al.* (1995). From the experimental data, our analysis allows the prediction and confirmation of the existence of an additional modification of the incommensurate  $\gamma$  phase.

## 2. The phase transitions and the C—Na bond formation

The structure of  $\text{Na}_2\text{CO}_3$  (Fig. 1) can be described as graphite-like layers formed by Na3 and  $\text{CO}_3$  ions, which are stacked along the hexagonal axis. Additional Na1,2 ions are located in the hexagonal channels. The graphite-like layers are regular in all modifications and all the C—Na3 bonds are characterized by the minimum temperature-independent distances,  $3.00 \pm 0.05$  Å (Fig. 2). The two other types of C—Na distances found in the hexagonal high-temperature  $\alpha$  phase are longer ( $\sim 3.4$  Å), pointing to weak interactions. One of them corresponds to the C—Na1,2 distance between the layer and

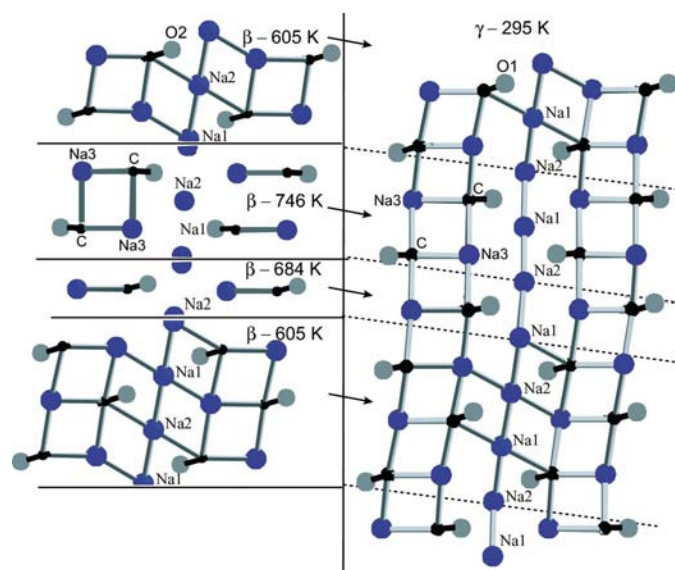


**Figure 3**

Analogy of the modulation wave and the temperature dependence in the  $\{110\}_{\text{hex}}$  family of planes. Interatomic distances smaller than 3.1 Å are shown by solid lines. The temperature-dependent evolution of the C—Na2 distance, Na3—C—Na3 angle and O2 displacement in the  $m_M$  plane in the  $\beta$  phase (left). Following the modulation along  $t$ , the same types of magnitudes occur again for C—Na1, Na3—C—Na3 angle and O1 displacement in the  $m_V$  plane along  $c$  in the  $\gamma$  phase (right).

channel atoms, the other corresponding to the interlayer C—Na3 distance. Both distances are located on a series of atomic planes parallel to  $\{110\}_{\text{hex}}$  (Fig. 1). In the hexagonal  $\alpha$  phase, these atomic planes correspond to the mirror planes  $m$ . In the monoclinic modifications, only one of the planes, namely  $m_M$  (Fig. 1), remains as a mirror plane. In this context, the other two are called  $m_V$  (virtual mirror) planes (Fig. 1).

Our analysis (Fig. 2) of the structural data shows that the series of phase transitions observed by decreasing temperature is associated with the formation of C—Na bonds in the family of  $\{110\}_{\text{hex}}$  atomic planes. The first step is the formation of bonds in the monoclinic  $m_M$  mirror plane. The second step is the formation of C—Na bonds in the two  $m_V$  planes of the incommensurate  $\gamma$  phase: two anti-phase waves of the C—Na distances appear respectively in two  $m_V$  planes along the internal  $t$  axis. The analogy of the temperature dependence

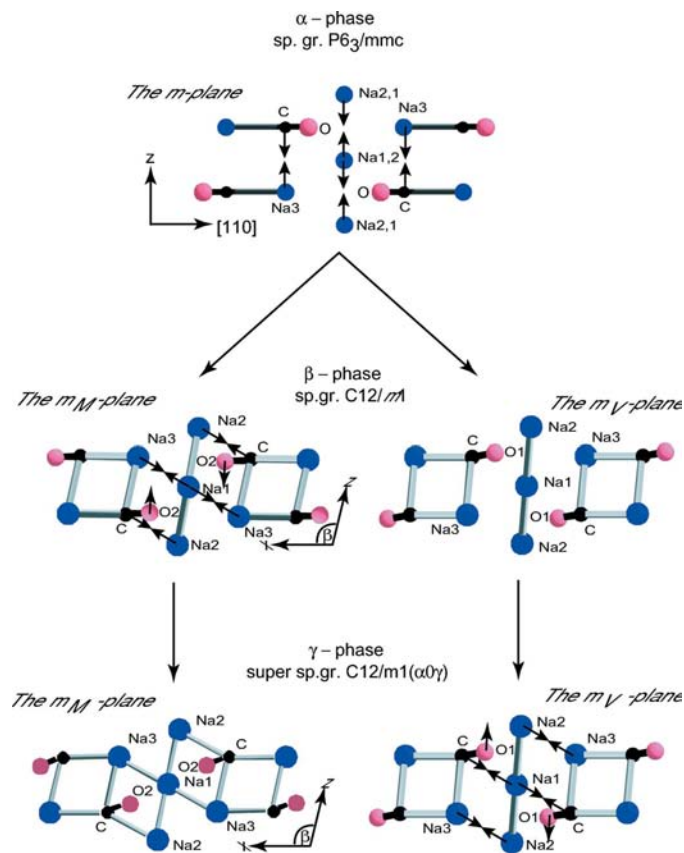


**Figure 4**

Phase transition scheme of  $\text{Na}_2\text{CO}_3$ . The structural transformations take place in the family of atomic planes  $\{110\}_{\text{hex}}$ . In the  $\alpha$  phase the interlayer C—Na3 distance decreases from 3.35 (972 K) to 3.23 Å (754 K). In the  $\beta$  phase significant changes appear on the mirror  $m_M$  plane: the decrease in the C—Na2 distances from 3.4 to 3.18 Å and C—Na3 from 3.23 to 3.1 Å induces an increase of the monoclinic  $\beta$  angle from 90 (754 K) to 99.33° (605 K); the decrease in the C—Na2 distance is associated with a shift of O2. In the  $\gamma$  phase significant transformations appear in the two  $m_V$  planes as anti-phase modes along  $t$ : the C—Na1 distances vary between 3.4 and 3.0 Å; the decrease of the C—Na1 distance is associated with a shift of O1. In the  $\gamma$  phase the content of the  $m_M$  plane is slightly affected by temperature: the monoclinic  $\beta$  angle changes only by 2.5° between 605 and 110 K; the convergence of the C—Na3 and C—Na2 distances also induces a convergence in the O2 atomic position.



and the modulation wave of the C–Na distances in the planes of the  $\{110\}_{\text{hex}}$  family is illustrated in Fig. 3. This analogy confirms the common nature of the C–Na interactions and points to a unique mechanism, inducing the sequence of phase transitions.

The structural transformation scheme is described in Fig. 4. A few remarkable features extracted from the distance–temperature diagrams of Fig. 2 should be underlined in this context.

(i) At the  $\alpha \rightarrow \beta$  transition, which occurs at 754 K, the interlayer distance C–Na3 = 3.23 Å splits into two distances, 3.1 and 3.35 Å, indicating a discontinuity in the structural transformation.

(ii) The shortest value matches the bond range and does not vary in the temperature range of the  $\beta$  phase. Another value reaches the bond range close to the  $\beta \rightarrow \gamma$  transition temperature of 605 K. At this temperature, the interlayer distance splits once more, varying from 3.1 to 2.9 Å along the internal  $t$  axis in the  $\gamma$  phase. This splitting again indicates a discontinuity of the structural transformation at 605 K.

(iii) In the temperature range of phase  $\beta$  the variation in the C–Na3 interlayer distances is independent of the continu-

ously decreasing C–Na2 distance, which causes the intensive increase of the monoclinic angle in the  $m_M$  plane (Fig. 4) that justifies the  $\epsilon_5 = a \cos \beta^* / a_0$  shear strain component.

(iv) This C–Na2 distance (3.18 Å at the transition temperature of 605 K) can still decrease in order to form a bond. This distance decreases continuously, reaching the bond value 3.1 Å only at  $\sim 530$  K (Fig. 2). At this temperature we can expect the splitting of the C–Na1 distance by anti-phase modulations in the  $m_V$  atomic planes. This occurs only after the formation of all the possible C–Na bonds in the  $m_M$  atomic plane.

Therefore, we propose an additional phase transformation at 530 K: incommensurate  $\gamma'$ –incommensurate  $\gamma$ . This is confirmed by the experimental X-ray diffraction pattern relating to the thermal treatment and the temperature dependence of the  $\alpha$  component of the  $\mathbf{q}$  vector, both published in de Wolff & Tuinstra (1986); Figs. 1 and 7, respectively. The IR spectra of the CO<sub>3</sub> group discussed below are also compatible with this assumption. The temperature-dependent modulation vector  $\mathbf{q}$  becomes rational,  $\mathbf{q} = \frac{1}{6}a^* + \frac{1}{3}c^*$ , at the  $\gamma$  to  $\delta$  transition. At this temperature, the commensurate ordering of the C–Na bonds results in a multiple monoclinic unit cell. In the lock-in  $\delta$  phase, the anti-phase modulation of the C–Na1 distances observed in the incommensurate phase freezes, resulting in three short ( $< 3.14$  Å) and three long ( $> 3.29$  Å) distances at 110 K. It can be expected that by further decreasing the temperature, the three shorter C–Na1 distances in the  $\delta$  phase will reach the shortest possible bond distances of  $3.0 \pm 0.1$  Å.

The evolution of the C–Na3 and C–Na1,2 distances is associated with the corresponding evolution of the Na1–Na2 and Na3–Na1,2 distances, as seen in Figs. 3 and 4. However, in contrast to the C–Na distances, the Na–Na distances decrease smoothly from 3.4 to 3.0 Å and do not show any specific characteristic of a phase transition.

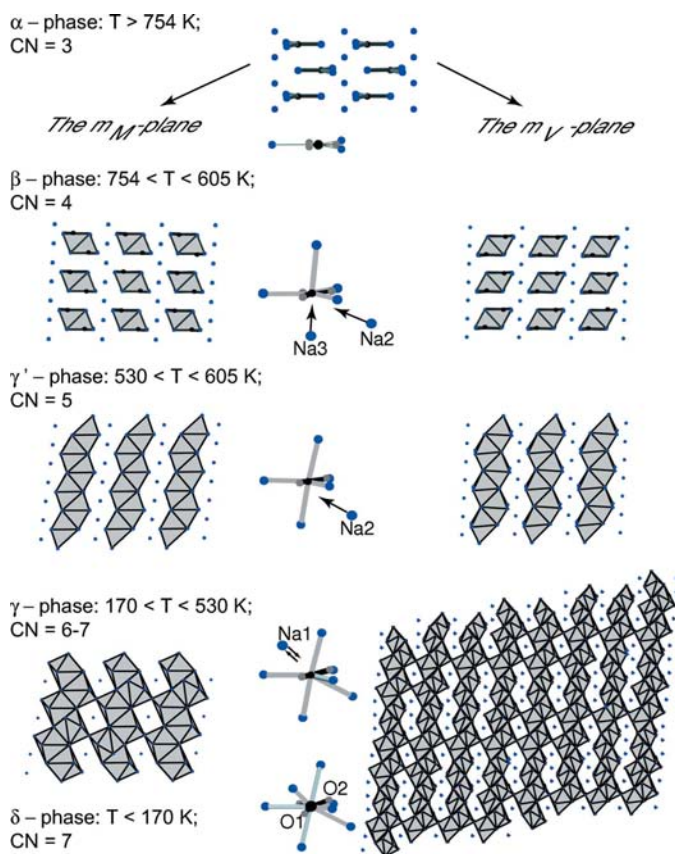


**Figure 5**  
Evolution of the Na environment in the vicinity of the C atom. The coordination number (CN) of the C atom is limited to the C–Na distances of up to 3.1 Å. The projections of  $[\text{CNa}_n]$  polyhedra are plotted in two different planes of the  $\{110\}_{\text{hex}}$  family. Non-bonded Na ions are shown by circles. The environment of the C atom including both Na ions and O atoms is also presented (center).

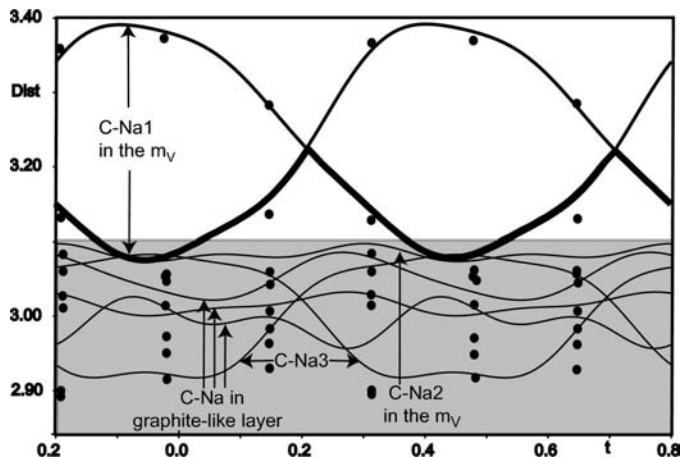


**Figure 6**  
 $t$ -dependence of the C–Na distances in the vicinity of the C atom in the  $\gamma$  (lines) and  $\delta$  (dots) phases. Six Na ions are always present in the second coordination sphere of C within the 3.1 Å radius (gray area). The bold line indicates the modulation of the seventh Na ion in the vicinity of C in the  $\gamma$  phase.

### 3. The Na environment of the C atom and the phase transition

The formation of the C—Na bonds which gradually appear on decreasing the temperature are associated with an increase in the number of Na ions in the vicinity of the C atoms, *i.e.* the coordination number (CN) of C in the second coordination sphere. In Fig. 5 the temperature-dependent evolution of the Na environment of the C atom within the 3.1 Å is projected on the  $m_M$  and  $m_V$  planes. Fig. 5 also indicates an increase in the plane density on decreasing the temperature.

It is significant that every additional bond formation (the increase of CN by 1) always relates to a new phase transition (Fig. 5, center). The three Na ions surrounding the C atom on the graphite-like layer correspond to CN = 3 in the  $\alpha$  phase. At 754 K, the  $\alpha \rightarrow \beta$  transition is characterized by a change of coordination number from 3 to 4 owing to the splitting of the interlayer C—Na3 distance. The  $\beta \rightarrow \gamma'$  transition temperature at 605 K increases the CN to 5. At 530 K, the  $\gamma' \rightarrow \gamma$  transition temperature, the CN increases to 6 owing to the formation of the C—Na2 bonds in the  $m_M$  atomic plane. An anti-phase modulation of two C—Na1 distances located on two  $m_V$  atomic planes appears at this temperature, thus producing domains of CN = 6 and a smaller fraction with CN = 7 in the incommensurate  $\gamma$  phase. The change in CN along the internal  $t$ -axis can be extracted from Fig. 6. At the  $\gamma \rightarrow \delta$  transition temperature, 170 K, the periodic sequence of CN (6, 6, 7) is realised once the modulation vector  $\mathbf{q}$  reaches  $[1/6, 0, 1/3]$  (Fig. 6). A complete stabilization of CN = 7 in the  $\delta$  phase can only be reached at lower temperature.

From this description, it can be concluded that in  $\text{Na}_2\text{CO}_3$  and by decreasing the temperature, the phase transitions are

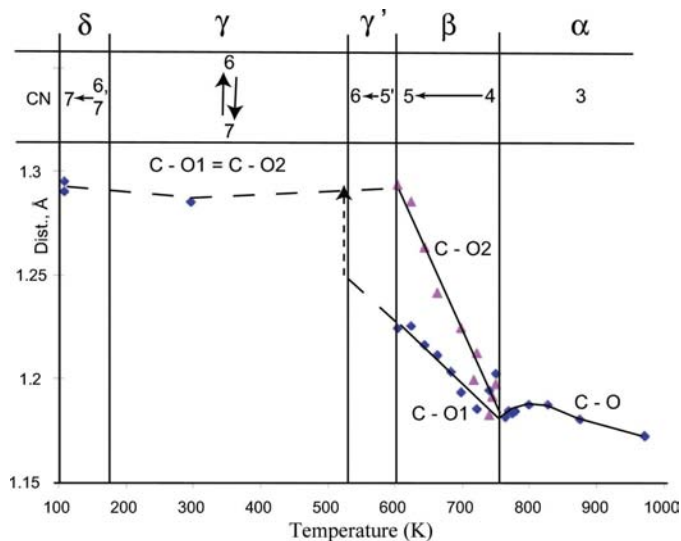


**Figure 7**

Correlation between the temperature dependences of the C—O distances (dots and lines) and the numbers of Na ions (CN) in the second coordination sphere ( $R = 3.1$  Å) of the C atom. Dashed lines are approximations. The C—O2 and C—O1 distances are located on the  $m_M$  respectively  $m_V$  planes. The distances are given without a libration correction.

characterized by an increase of the number of C—Na bonds (respectively CN) in the second coordination sphere of the C atoms. Knowing that the intralayer bonds are constant over the whole temperature range, this number increases owing to the strengthening of both interlayer C—Na3 interactions and interactions between the layers and the channel atoms, Na1 and Na2. None of the channel atoms are bonded in the  $\alpha$  phase, whereas they are completely bonded to the C atom in the lowest  $\delta$  phase.

Taking into account the crystallographic analogy between C and Na3 (Fig. 1), we can state that the phase transitions are linked to an increase in the non-O atom concentration close to the intersections of the most densely packed atomic planes, namely the graphite-like layers [the (001) planes] and the three planes of the  $\{110\}_{\text{hex}}$  family. Both C and Na3 are located at these intersections. At each intersection and within 3.1 Å, the non-O-atom concentration increases on decreasing the temperature: in the graphite-like layer of the  $\alpha$  phase (754–972 K) only one atom can be found within this radius. In the  $\beta$  phase (605–754 K) the number increases to two owing to the interlayer contacts. The concentration increases from 2 to 2.5

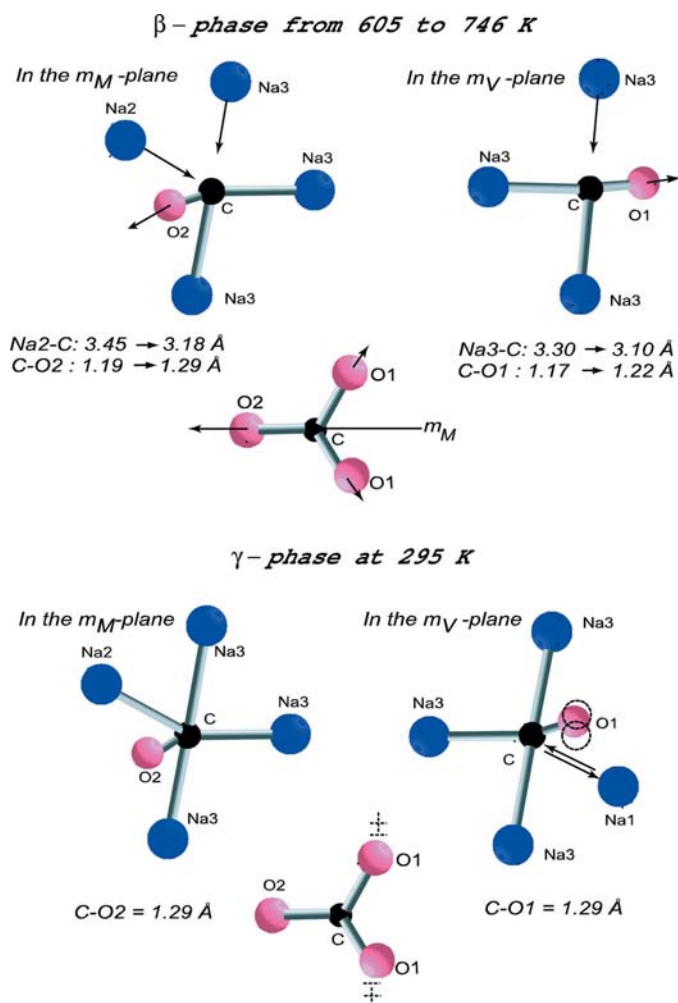


**Figure 8**

Correlation between the first (O atoms) and the second (Na ions) coordination spheres of C in the  $\beta$  and  $\gamma$  phases.

atoms, which corresponds to the progressive deformation of the atomic arrangement on the  $m_M$  plane of the  $\gamma'$  phase (530–605 K). A modulation of the concentration from 2.5 to 3 atoms appears in the  $\gamma$  phase owing to the atomic arrangement on the  $m_V$  planes (170–530 K). At 110 K, the  $\delta$  phase, we find an ordered sequence of atom concentration (2.5, 2.5, 3) aligned along  $\mathbf{q}$ . We postulate a value of 3 for the atom concentration as a limiting value at the lowest temperature of the  $\delta$  phase.

#### 4. Influence of the Na environment on the CO<sub>3</sub> group

The temperature dependence of the Na environment of the C atom is correlated to both a tilt of the CO<sub>3</sub> group (Fig. 5) and the C–O distances (Fig. 7). This correlation is illustrated in Fig. 8. The O atoms attempt to avoid the screening for the C–Na interactions. This is why the O atom deviates gradually from the C–Na line in the corresponding plane (Fig. 3–5 and 8). As a consequence, we observe a tilt of the CO<sub>3</sub> triangle. As can be deduced from Fig. 8, the increase of the C–Na bond number and the associated decrease of the bond length induces an increase of the C–O distances in the family of atomic planes {110}<sub>hex</sub> (Fig. 7). Therefore, the difference between the C–O1 (in  $m_V$ ) and C–O2 (in  $m_M$ ) distances, the very large anisotropy of their thermal libration (discussed by Wolff & Tuinstra, 1986, for  $\alpha$  and  $\beta$  phases), and the difference in the  $t$ -dependent displacements between O1 and O2 revealed by Dušek *et al.* (2003) are a direct consequence of the lengths and numbers of C–Na bonds. In other words, the carbonate group is not a fully rigid unit. Moreover, the

complex IR absorption spectra of the internal modes of the carbonate ion revealed in Harris & Salje (1992) are also directly correlated with the CN of the C atom (Fig. 5 and 9).

#### 5. Conclusions

We have established a direct link between the C–Na distances and the sequence of phase transformations in Na<sub>2</sub>CO<sub>3</sub>, which is systematic over the full range of phases. By decreasing the temperature, the consecutive increase of the C–Na bond number (CN) in the second coordination sphere of the C atom as 3 → 4 → 5 → 6–7 → 7 fits respectively the  $\alpha \rightarrow \beta \rightarrow \gamma'$  (predicted) →  $\gamma \rightarrow \delta$  phase transitions. This is the main conclusion of the present work. Consequently, we propose to directly associate the C–Na bond formation with the phase transition mechanism:

(i) The  $\alpha \rightarrow \beta$  phase transition which appears at 754 K is characterized by a splitting of the C–Na3 = 3.23 Å interlayer distance ( $\alpha$  phase) into 3.1 and 3.35 Å ( $\beta$  phase). This splitting clearly defines the internal structure discontinuity, but does not affect the lattice parameters and, therefore, cannot be characterized by or be caused by any spontaneous shear strain, including  $\epsilon_5$  discussed by Swainson *et al.* (1995) for Na<sub>2</sub>CO<sub>3</sub> as the primary order parameter of the second-order ferroelastic  $\alpha \rightarrow \beta$  phase transition. However, this interlayer C–Na3 bond formation can be a reason for the widely discussed ‘lattice melting’ observed at the phase transition (Swainson *et al.*, 1995; Harris & Dove, 1995, Harris *et al.*, 1996). Therefore, the  $\alpha \rightarrow \beta$  phase transition needs a more consistent interpretation.

(ii) The  $\beta \rightarrow \gamma'$  transformation is a first-order phase transition of the commensurate–incommensurate type at 605 K. The appearance of modulations affects the interlayer C–Na3 distances; no significant modulation of the C–Na1 distances can be observed.

(iii) We propose a new incommensurate–incommensurate phase transition,  $\gamma' \rightarrow \gamma$  at ~ 530 K. This transition is associated with the creation of a high-amplitude anti-phase modulation of C–Na1 distance in two planes of the (110)<sub>hex</sub> family.

(iv) The  $\gamma \rightarrow \delta$  ‘incommensurate–lock-in’ transformation is related to the ordering of the C–Na1 bonds in three-dimensional space.

This work is supported by the Swiss National Science Foundation, grant Nos. 20-67698.02 and 200021-109470. M. Dušek is also gratefully acknowledged for his kind help.

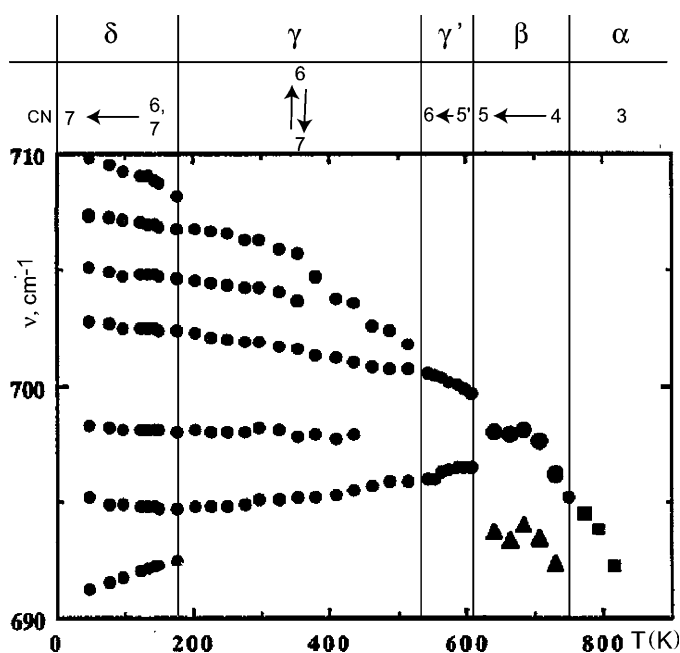


**Figure 9**  
Correlation between the IR spectra of the CO<sub>3</sub> internal modes (after Harris & Salje, 1992) and the Na environment of the C atom at different temperatures. The solid vertical lines correspond to the phase-transition temperatures.

#### References

- Dušek, M., Chapuis, G., Meyer, M. & Petříček, V. (2003). *Acta Cryst.* **B59**, 337–352.  
 Harris, M. J. & Dove, M. T. (1995). *Modern Phys. Lett. B*, **9**, 67–85.  
 Harris, M. J., Dove, M. T. & Godfrey, K. W. (1996). *J. Phys. Condens. Matter*, **8**, 7073–7084.

- Harris, M. J. & Salje, K. H. (1992). *J. Phys. Condens. Matter*, **4**, 4399–4408.
- Hemmersbach, S., Zibrowius, B. & Ruschewitz, U. (1999). *Z. Anorg. Allg. Chem.* **625**, 1440–1446.
- Parlinski, K. & Chapuis, G. (1993). *Phys. Rev. B*, **47**, 13983–13991.
- Swainson, I. P., Dove, M. T. & Harris, M. J. (1995). *J. Phys. Condens. Matter*, **7**, 4395–4418.
- Wolf, P. M. & Tuinstra, F. (1986). *Incommensurate Phases in Dielectrics*, edited by R. Blinc & A. P. Levanyuk, Vol. 2, pp. 253–281. Amsterdam: North-Holland-Elsevier.